

The answer to concerted versus step-wise controversy for the double proton transfer mechanism of 7-azaindole dimer in solution

Satoshi Takeuchi and Tahei Tahara[†]

Molecular Spectroscopy Laboratory, RIKEN (The Institute of Physical and Chemical Research), 2-1, Hirosawa, Wako 351-0198, Japan

Edited by Nicholas J. Turro, Columbia University, New York, NY, and approved January 12, 2007 (received for review November 20, 2006)

The dynamics and mechanism of the double proton transfer reaction of the 7-azaindole dimer was investigated in solution by excitation wavelength dependence in steady-state and femtosecond time-resolved fluorescence spectroscopy. Femtosecond measurements in the UV region revealed that the dynamics of the dimer fluorescence exhibits remarkable change as the excitation wavelength was scanned from 280 to 313 nm. The fluorescence showed a biexponential decay (0.2 and 1.1 ps) with 280-nm excitation, whereas it exhibited a single exponential decay (1.1 ps) with 313-nm excitation (the red-edge of the dimer absorption). This observation clearly indicates that the 0.2-ps component is irrelevant to the proton transfer. In the visible region, we found that the tautomer fluorescence rises in accordance with the decay of the dimer fluorescence with a common time constant of 1.1 ps. This finding unambiguously denies the appearance of any intermediate species in between the dimer and tautomer excited states, indicating that the double proton transfer reaction is essentially a single-step process. We conclude that the double proton transfer of the 7-azaindole dimer in solution proceeds in the concerted manner from the lowest excited state with the 1.1-ps time constant. On the basis of the experimental data obtained, we discuss the long-lasting concerted versus step-wise controversy for the double proton transfer mechanism in solution.

femtosecond spectroscopy | fluorescence | ultrafast | photochemistry

Excited-state proton transfer has been receiving a great deal of attention, because it plays crucial roles in photochemistry and photobiology (1–3). The doubly hydrogen-bonded dimer of 7-azaindole is a prototypical system showing such a reaction in the photoexcited state. This dimer has served as one of the most central model systems, and hence its photochemistry and photophysics have been extensively studied for more than three decades (4–18). Spectroscopic measurements revealed that the 7-azaindole dimer exhibits a double proton transfer reaction after photoexcitation (Fig. 1) (4–7, 9, 10). The reactive nature of the 7-azaindole dimer in hydrocarbon solvent is manifested by its steady-state fluorescence spectrum, which shows significantly red-shifted fluorescence attributed to the tautomer fluorescence. The steady-state fluorescence spectra that were examined under various conditions provided information about photochemical properties of the relevant excited states (5, 6, 9, 10). The proton transfer time was first reported as <5 ps in 1979 by picosecond fluorescence spectroscopy (14), and then it was determined as 1.4 ps by measuring the rise of the tautomer fluorescence with femtosecond time resolution (15).

A fundamental question relevant to this ultrafast double proton transfer is the cooperativity of the motion of the two protons. So far, it has been intensively argued whether the two protons move in a concerted or step-wise way. The head-on arguments on this mechanism were first made on the basis of time-resolved data for the reaction occurring in a supersonic jet. Douhal *et al.* (19) observed a biexponential feature in time-resolved ion signals of femtosecond pump-probe mass spectroscopy. They associated the biexponential transients with the

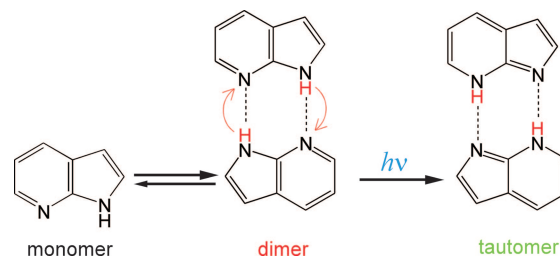


Fig. 1. Photoinduced double proton transfer reaction of 7-azaindole dimer.

step-wise motion of the two protons and assigned the two components to the dimer excited state and zwitterionic intermediate species, respectively. In other words, they claimed that the proton-transfer dynamics intrinsically shows biexponential behavior with appearance of the intermediate species in which only one proton is transferred (the step-wise mechanism). A similar conclusion was also given by femtosecond Coulomb explosion experiments (20).

To elucidate the reaction dynamics and mechanism in the solution phase, we carried out systematic femtosecond fluorescence measurements for the 7-azaindole dimer in a nonpolar solvent (16, 21). We found that the fluorescence from the dimer excited state (before the proton transfer) shows a biexponential decay with time constants of 0.2 and 1.1 ps, when the dimer is excited at the high-energy side of the absorption band. On the basis of quantitative analysis (time-resolved spectra, transition-moment directions, and oscillator strengths), we concluded that the 0.2-ps component corresponds to the 1L_b (S_2) \rightarrow 1L_a (S_1) electronic relaxation and that the 1.1-ps component corresponds to the double proton transfer taking place from the 1L_a state (16). In other words, we concluded that the proton-transfer process itself shows a single exponential behavior, corresponding to the cooperative translocation of the two protons (the concerted mechanism). Following our work, Fiebig and colleagues (22, 23) also reported their femtosecond fluorescence and absorption study in solution and confirmed the existence of the two components. However, they interpreted the existence of the two components as manifestation of the step-wise double proton transfer in solution, as originally proposed for the reaction in the gas phase.

The two different interpretations for femtosecond dynamics of the 7-azaindole dimer in solution triggered very intense

Author contributions: S.T. and T.T. designed research, performed research, analyzed data, and wrote the paper.

The authors declare no conflict of interest.

This article is a PNAS Direct Submission.

[†]To whom correspondence should be addressed. E-mail: tahei@riken.jp.

This article contains supporting information online at www.pnas.org/cgi/content/full/0610141104/DC1.

© 2007 by The National Academy of Sciences of the USA

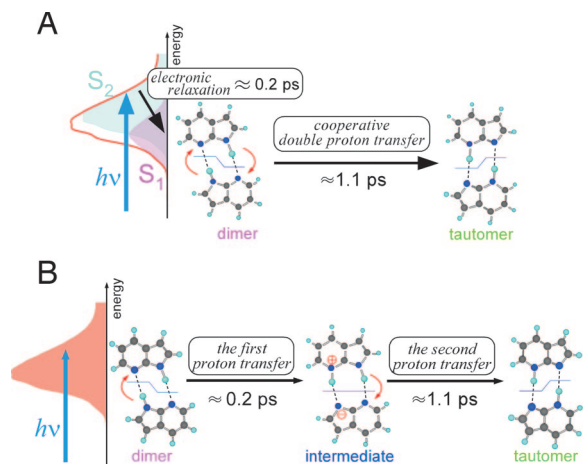


Fig. 2. Two mechanisms proposed for the double proton transfer reaction of the 7-azaindole dimer. (A) Concerted mechanism. (B) Step-wise mechanism.

debates, and the mechanism of the double proton transfer has been a central issue of the discussion (17, 24–33). Detailed theoretical calculations for the excited-state potential energy surface along the proton transfer coordinate have been performed to examine the existence of a local minimum corresponding to the intermediate species (24, 30, 34–36). However, the calculated results depend sensitively on the symmetry and excited-state geometry of the dimer, which makes it difficult to derive a definitive conclusion.

From the viewpoint of experiments, assignments of the 0.2- and 1.1-ps components are the key to resolve the controversy between these two interpretations. Previously, we proposed that changing the excitation wavelength in time-resolved fluorescence measurements can experimentally differentiate the two reaction mechanisms (37). This proposal is based on the fact that the initial population of the S_1 and S_2 states changes by the shift of the excitation wavelength. Therefore, if the concerted mechanism is operative, significant change of the relative amplitude of the 0.2- and 1.1-ps components is expected (Fig. 2A). In contrast, if the step-wise mechanism is the case, such a change should not be seen, because the relative amplitude is determined by the inherency of the two successive steps starting from a single dimer excited state (Fig. 2B).

In this paper, we present a full account of our study for the excitation-wavelength dependence of the fluorescence dynamics of

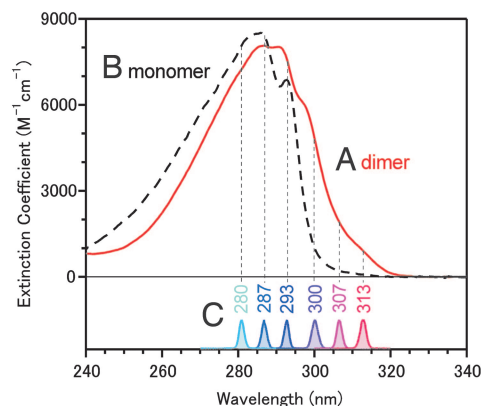


Fig. 3. Excitation condition of the present femtosecond fluorescence experiment. Absorption spectra of the 7-azaindole dimer (Spectrum A) and monomer (Spectrum B). Spectrum C are of the six excitation pulses used in the present study.

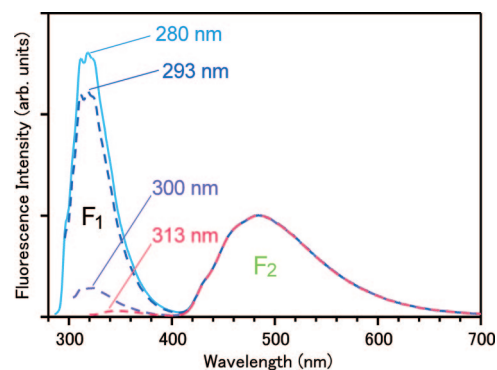


Fig. 4. Steady-state fluorescence spectra of 7-azaindole in hexane (1×10^{-2} mol \cdot dm $^{-3}$) measured at room temperature with four excitation wavelengths. These spectra were normalized by the peak intensity of the F₂ band after correction for the instrumental sensitivity and reabsorption of the sample.

the 7-azaindole dimer in solution. Our measurements revealed that the fluorescence dynamics shows significant excitation wavelength dependence. Furthermore, the tautomer fluorescence showed a single exponential rise in full accordance with a single exponential decay of the dimer fluorescence when the dimer is excited at the red-edge of the absorption band. On the basis of these time-resolved fluorescence data, we discuss the cooperativity of the motion of the two protons in solution.

Results and Discussion

Steady-State Spectroscopic Properties of 7-Azaindole. In concentrated nonpolar solvents, the greater part of 7-azaindole molecules are present as the dimer. The monomer–dimer equilibrium was examined in detail by analyzing the concentration dependence of absorption spectra (6, 16). It was concluded (16) that 86.8% of the 7-azaindole molecules are present as the dimer in room-temperature hexane solution with a concentration of 1×10^{-2} mol \cdot dm $^{-3}$, which we used in the present study. Fig. 3 shows the absorption spectra of the monomer and dimer that were obtained by the spectral decomposition procedure taking account of this monomer–dimer equilibrium. The lowest-energy absorption band of the 7-azaindole dimer is red-shifted by ≈ 10 nm with respect to the monomer band. Thus, it is readily understood that the dimer can be preferentially photoexcited with wavelengths of >300 nm.

In the present study, we used six excitation wavelengths between 280 and 313 nm. As shown in Fig. 3C, these excitation wavelengths cover a principal portion of the dimer absorption, including the red-edge of the absorption band (313 nm). Steady-state fluorescence spectra obtained with four selected excitation wavelengths are depicted in Fig. 4. The steady-state fluorescence of the concentrated solution shows a dual band spectrum in the UV–visible region. The band in the visible region (F₂ band; $\lambda_{\max} = 490$ nm) is due to the 7-azaindole dimer and has been assigned to the fluorescence from the tautomer excited state generated by the proton transfer reaction (5). The other band in the UV region (F₁ band; $\lambda_{\max} = 320$ nm) arises from the coexisting monomer that does not show any reactivity. The relative intensity of the F₁ and F₂ bands changes drastically with the shift of the excitation wavelength, reflecting the absorption difference between the dimer and the monomer. However, the spectral shape of the F₂ band does not change at all with the excitation wavelength. In fact, when we normalize the fluorescence spectra by the F₂-band intensity, they overlap perfectly with one another in the visible region, as shown in Fig. 4. This result assures us that the proton transfer reaction of the 7-azaindole dimer takes place regardless of the change of the excitation wavelength, including the red-edge excitation at 313 nm.

We note that the fluorescence spectrum obtained with 313-nm

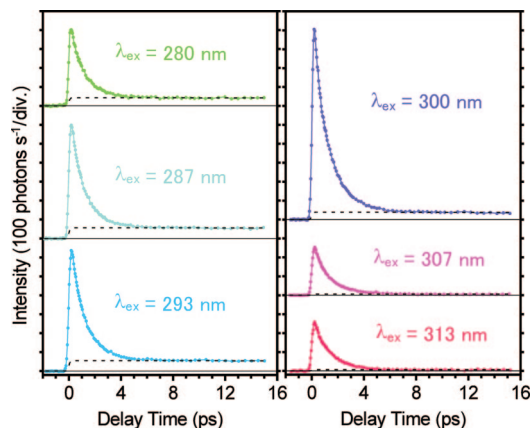


Fig. 5. Femtosecond time-resolved fluorescence signals of 7-azaindole in hexane (1×10^{-2} mol·dm $^{-3}$) measured at 380 nm with six excitation wavelengths. The dotted curve drawn for each trace represents a calculated temporal change of the monomer fluorescence.

excitation showed a very weak band at ≈ 350 nm [supporting information (SI) Fig. 10]. This band is not assignable to the dimer fluorescence (before the reaction) but is attributed to small amount of aggregate formed in solution (38), which absorbs more in the red (see *SI Text* for details). The dimer fluorescence is noticeable only in femtosecond time-resolved measurements, which we discuss below.

Excitation Wavelength Dependence of the UV Fluorescence Dynamics.

Femtosecond time-resolved fluorescence signals of 7-azaindole in hexane are shown in Fig. 5 for six excitation wavelengths. The fluorescence emission was monitored at 380 nm, where the fluorescence from the dimer excited state(s) (before the reaction) predominantly contributes to the signal. Therefore, the rapid decay observed in several picoseconds is directly related to the dynamics of the dimer excited state in question. Additionally, a weak component also is seen as an almost flat tail in each time-resolved trace. This long-lived component comes from the monomer that coexists in the solution. Its relative amplitude varies, reflecting the absorption difference between the monomer and dimer at each excitation wavelength. Thus, the time-resolved signals in Fig. 5 contain the fluorescence from the dimer excited state(s) (the dimer fluorescence) and a small contribution from the coexisting monomer (the monomer fluorescence).

To quantitatively analyze the dynamics of the dimer fluorescence, we subtracted the monomer component from the raw data. For this purpose, we represented the monomer component by a single exponential function with its lifetime of 1 ns (16) and fitted it to the raw data by the tail-matching method (Fig. 5, dotted curves). The dimer fluorescence obtained after subtraction is plotted in Fig. 6*A* for the three excitation wavelengths. Clearly, the dynamics of the dimer fluorescence shows significant excitation wavelength dependence, especially in the early time region. To examine this dependence in more detail, we plot the dimer fluorescence in a logarithmic scale in Fig. 6*B*. All of the decay curves were well fitted by a biexponential function with time constants of $\tau_1 = 0.2 \pm 0.1$ ps and $\tau_2 = 1.1 \pm 0.1$ ps (Table 1). The dotted straight line represents the 1.1-ps component, and hence the deviation from this line, which is recognized in the early time, corresponds to the 0.2-ps component. Obviously, the excitation wavelength dependence comes from the change of the relative amplitude between the 0.2- and 1.1-ps components. In fact, a biexponential feature is pronounced when the dimer is excited by short-wavelength light (280 and 287 nm), being consistent with our previous results obtained with 270-nm

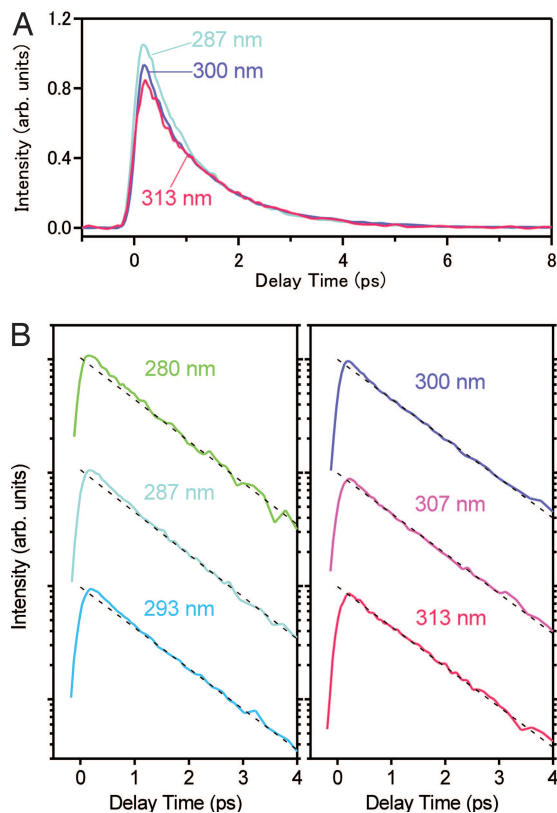


Fig. 6. Comparison of the temporal changes of the dimer fluorescence. (A) Linear plot of the temporal changes of the dimer fluorescence obtained with 287-, 300-, and 313-nm excitation. (B) Logarithmic plot of the temporal changes of the dimer fluorescence for the six excitation wavelengths. The dotted straight line drawn for each trace corresponds to the 1.1-ps single exponential decay.

excitation (16, 21). In contrast, however, as the excitation wavelength becomes longer, the relative amplitude of the 0.2-ps component becomes significantly smaller. Eventually, the 0.2-ps component completely vanishes when the red-edge of the dimer absorption (313 nm) is excited, and the dimer fluorescence shows a single exponential decay (1.1 ps). These results suggest that only the lowest excited state of the dimer is selectively populated by the red-edge excitation and that it exhibits a single exponential decay as the proton transfer reaction takes place.

To confirm the selective photoexcitation of the lowest excited state, we compared femtosecond fluorescence anisotropy at 380 nm obtained with 313- and 270-nm excitations (Fig. 7). The anisotropy obtained with the 270-nm excitation shows a fast, ≈ 0.2 -ps component in addition to a slow, ≈ 12 -ps component

Table 1. Fitting parameters (amplitudes) for fluorescence decays at 380 nm as a function of excitation wavelength (λ_{ex})

λ_{ex} , nm	A_1	A_2	A_m	A_1/A_2
280	132	378	43.0	0.35
287	173	580	56.8	0.30
293	133	648	55.5	0.21
300	294	1,020	38.7	0.29
307	25.1	279	5.8	0.090
313	3.7	292	6.5	0.013

Values under A_1 indicate amplitudes of the 0.2-ps component, values under A_2 indicate amplitudes of the 1.1-ps component, and values under A_m indicate amplitudes of the monomer component.

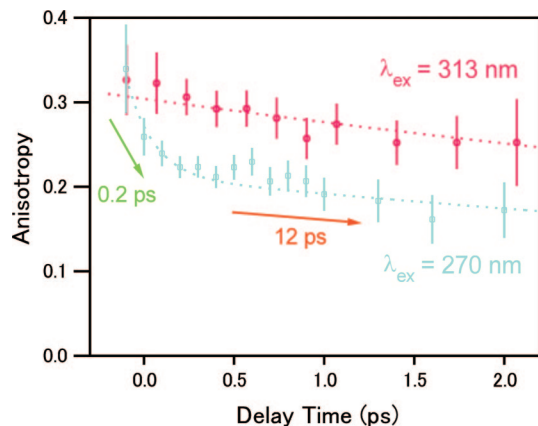


Fig. 7. Femtosecond fluorescence anisotropy data of 7-azaindole in hexane (1×10^{-2} mol·dm $^{-3}$) measured at 380 nm with 270- and 313-nm excitation.

that is due to the orientational diffusion of the 7-azaindole dimer in hexane (16). The fast component cannot be assigned to the orientational diffusion, because the molecular motion is negligible in such a short time region. Because the fast component decays correspondingly with the 0.2-ps component of the fluorescence intensity data, it was assigned to the change of the electronic state ($S_2 \rightarrow S_1$ internal conversion) that rotates the transition-moment direction of the fluorescence (16). In sharp contrast, the anisotropy obtained with the red-edge excitation shows essentially a single exponential decay corresponding to the orientational diffusion. This absence of the fast component strongly indicates that the change of the electronic state does not take place. Thus, in the case of the red-edge excitation, we can conclude that the fluorescence at 380 nm is emitted only from the initially populated state, i.e., the lowest excited state (S_1) of the dimer.

Excitation Wavelength Dependence of the Visible Fluorescence Dynamics. On the basis of the femtosecond fluorescence intensity/anisotropy data in the UV region, we conclude that only the lowest excited state of the 7-azaindole dimer is selectively populated by the red-edge excitation and that it disappears with the 1.1-ps time constant as the proton transfer reaction proceeds. In addition to this dimer excited-state dynamics, the formation dynamics of the tautomer excited state (the product) also is important to a discussion of the reaction mechanism.

Fig. 8 shows femtosecond time-resolved fluorescence signals in the visible region after the dimer was most preferentially excited by 313-nm light. At 560 nm, a long-lived component with a finite rise time is observed. This component is assignable to the fluorescence from the tautomer excited state generated by the proton transfer reaction [the tautomer fluorescence, 3.2-ns lifetime (16)], because this wavelength region corresponds to the F_2 band. At 420 nm, the observed signal shows a rapidly decaying feature in the first several picoseconds, although a small contribution from the tautomer fluorescence also is seen. The rapid decay is attributable to the dimer fluorescence that extends into the visible region (16, 21). This assignment is confirmed in Fig. 9, where we normalized the fluorescence signals at 420 and 560 nm by the tail-matching method and calculated the difference of the two. The tautomer component contained in the two (normalized) signals was cancelled in this procedure, leaving other components only. Clearly, the difference signal shows a single exponential behavior with a time constant of 1.2 ps, as seen in the logarithmic plot (Fig. 9 *Inset*). This time constant coincides with that of the dimer fluorescence ($\tau_2 = 1.1 \pm 0.1$ ps), which is within our experimental error. Therefore, the rapid decay at 420

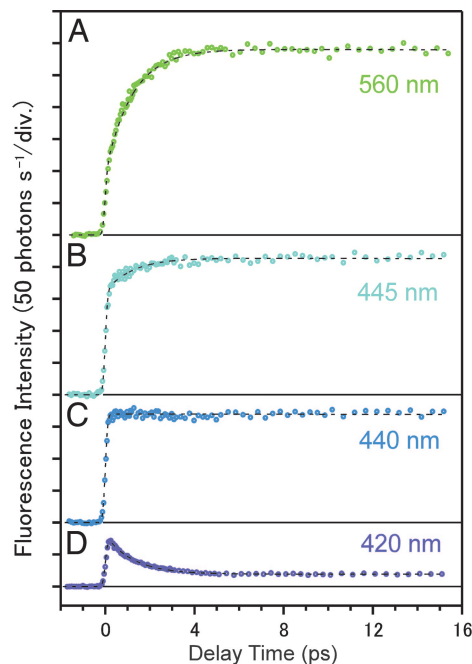


Fig. 8. Femtosecond time-resolved fluorescence signals of 7-azaindole in hexane (1×10^{-2} mol·dm $^{-3}$) monitored at four visible wavelengths after 313-nm excitation.

nm arises from the dimer fluorescence. More importantly, the single exponential behavior strongly indicates that the time-resolved fluorescence signals in Fig. 8 contain only two components, i.e., the 1.1-ps dimer fluorescence and the long-lived tautomer fluorescence. In other words, only the fluorescence signals from the precursor and product excited states are observed. Fluorescence from other excited states, such as intermediate species, does not appear.

The rise time of the tautomer fluorescence (τ_r) can be evaluated

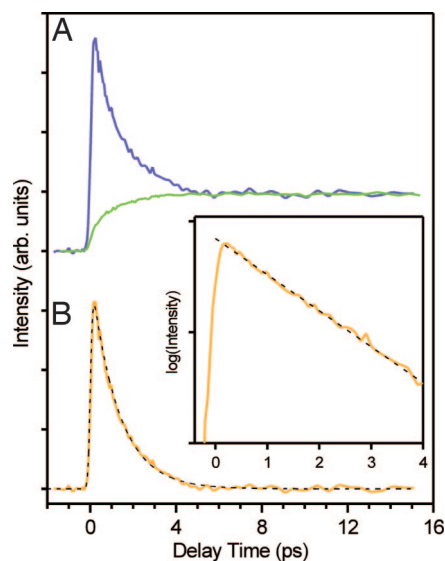


Fig. 9. Decomposition of the time-resolved fluorescence signals in the visible region. (A) Time-resolved fluorescence signals at 420 and 560 nm after tail-matching normalization. (B) Temporal behavior of the difference signal between the two normalized traces and a calculated single exponential decay with a time constant of 1.2 ps (dashed curve). (*Inset*) A logarithmic plot of the difference signal.

directly from the time-resolved signal at 440 nm without any fitting analysis. A flat feature is seen over the entire time region at 440 nm (Fig. 8C), which indicates that the rise of the tautomer fluorescence is completely cancelled by the decay of the dimer fluorescence at this particular wavelength (i.e., isoemissive point). Therefore, the rise time of the tautomer fluorescence is uniquely determined to be the same as the decay time constant of the dimer fluorescence, $\tau_r = \tau_d = 1.1 \pm 0.1$ ps. This argument is supported by the observation of the rising and decaying feature at wavelengths longer and shorter than 440 nm, respectively, reflecting the gradual change in the relative contributions of the dimer and tautomer fluorescence. We note that the same rise time ($\tau_r = 1.1$ ps) also was obtained by fitting analysis using the two components, which perfectly reproduced the time-resolved signals, as shown by the dotted curves in Fig. 8.

From these results of femtosecond fluorescence measurements in the visible region, we conclude that the tautomer fluorescence appears in accordance with the disappearance of the dimer fluorescence with the common 1.1-ps single exponential behavior (see also *SI Text* and *SI Fig. 11*). Obviously, these results strongly deny the appearance of any noticeable intermediate in between the dimer and tautomer excited states.

Mechanism of the Double Proton Transfer Reaction of the 7-Azaindole Dimer. The excitation-wavelength dependence of the fluorescence of the 7-azaindole dimer gives firm grounds to experimentally distinguish the two mechanisms and to solve the long-lasting controversy.

If the step-wise mechanism is operative, the excited dimer first undergoes a single-proton transfer to become the intermediate species, in which only one proton is transferred. Then, the intermediate species is converted to the tautomer by the second single-proton transfer. As illustrated in Fig. 2B, the 0.2- and 1.1-ps components correspond to the appearance and disappearance of the intermediate species. Therefore, the biexponential feature of the time-resolved fluorescence is inherent to the proton transfer process itself, and, moreover, the relative amplitude of the two components should not change significantly by the change of the excitation wavelength. However, this expectation is not consistent with the present experimental result, which demonstrated that the relative amplitude of the 0.2-ps component shows significant excitation-wavelength dependence. More crucially, the absence of the 0.2-ps component in the time-resolved fluorescence with the red-edge excitation indicates that the 0.2-ps component has no relation with the proton transfer reaction itself. It is clear that the step-wise mechanism never accords with the observed femtosecond fluorescence dynamics.

In the context of the concerted mechanism, the 0.2-ps component is assigned to the $S_2 \rightarrow S_1$ internal conversion in the excited dimer, whereas the 1.1-ps component is assigned to the concerted double proton transfer process. The excitation-wavelength dependence observed is readily explained by this concerted mechanism. In the 7-azaindole dimer, the absorption spectra due to the $S_1 \leftarrow S_0$ and $S_2 \leftarrow S_0$ transitions considerably overlap each other, forming the lowest-energy absorption band in solution (see *SI Text*, *SI Fig. 12*, and *SI Table 2* for the electronic structure of the excited dimer). However, because the $S_2 \leftarrow S_0$ transition is located in a slightly higher-energy region, the S_2 state is generated more efficiently than the S_1 state by the short-wavelength excitation. Therefore, the 0.2-ps component, which reflects the population of the S_2 state, is prominently observed. As the excitation wavelength becomes longer, the efficiency of the generation of the S_2 state becomes lower, and hence, the relative amplitude of the 0.2-ps component also becomes smaller. Eventually, when the red-edge of the dimer absorption is photoexcited, only the S_1 state is selectively populated, so that the dynamics corresponding to the $S_2 \rightarrow S_1$ internal conversion does not appear. This situation is fully consistent with the

present time-resolved fluorescence data. In fact, the relative amplitude of the 0.2-ps component in the dimer fluorescence became smaller as the excitation wavelength became longer. The selective excitation of the S_1 state was confirmed by the absence of the fast component (≈ 0.2 ps) in time-resolved fluorescence anisotropy data. Thus, the excitation-wavelength dependence of the femtosecond fluorescence dynamics directly supports the concerted mechanism.

The time-resolved fluorescence data obtained with the red-edge excitation reveal that the proton transfer reaction starts from the S_1 state of the dimer with the 1.1-ps time constant. Furthermore, the decay of the dimer fluorescence accords with the rise of the tautomer fluorescence with the common time constant of 1.1 ps. This result denies the appearance of any intermediate in between the dimer and the tautomer excited states, and hence it means that the tautomer excited state is directly generated from the S_1 state of the dimer. In other words, the double proton transfer is inherently a single-step process from the viewpoint of experiments. Consequently, we can conclude that the double proton transfer reaction of the 7-azaindole dimer in solution proceeds in the concerted manner from the S_1 state of the dimer with the 1.1-ps time constant.

It is worth mentioning the recent progress in the study of the double proton transfer reaction in the gas phase, because the step-wise mechanism was originally proposed based on results of the gas-phase experiments. Douhal *et al.* (19) investigated the reaction of the jet-cooled 7-azaindole dimer by femtosecond pump-probe mass spectroscopy and observed a biexponential feature in the temporal behavior of the ion signals. They interpreted the biexponential decay as a manifestation of the step-wise transfers of the two protons. A support for this interpretation was given by Castleman and coworkers (20), who detected 7-azaindole+H⁺ mass-119 species after photoexcitation of the 7-azaindole dimer in the Coulomb explosion experiment. Recently, this interpretation of the gas-phase experiments was questioned by a series of works by Sakota and Sekiya and their coworkers (39–42). They measured fluorescence excitation and hole-burning spectra of the jet-cooled 7-azaindole dimer in the S_1 – S_0 region and showed that the bandwidth of each vibronic band is largely different, depending on the vibrational mode (39). This result indicates a vibrational-mode-specific proton transfer rate, which was actually reported first in the 1980s (11, 13). Sakota *et al.* (39) concluded that the biexponential decay observed in the femtosecond gas-phase experiments is caused by the simultaneous excitation of these closely located vibronic states having different reaction rates. Actually, in a later work (42), they selectively excited each vibronic state using narrow-band picosecond pulses and clearly observed single exponential decays of time-resolved resonance-enhanced multiphoton ionization signals. Moreover, they measured dispersed fluorescence spectra of three isotopomers (7-azaindole-hh, -hd, -dd), and evaluated the proton (deuteron) transfer rates from the relative intensity of the dimer and tautomer bands (41). It was found that the proton (deuteron) transfer rate varies quite asymmetrically with respect to the deuteration content ($k^{\text{hh}}/k^{\text{hd}} \approx 60$ and $k^{\text{hd}}/k^{\text{dd}} \approx 12$) and that the excitations of the undeuterated and deuterated moieties in 7-azaindole-hd gave comparable rates ($k^{\text{h*d}} \approx k^{\text{hd*}}$). This finding means that the deuterium effect on the motion of the two protons cannot be considered separately, i.e., that the double proton transfer has a cooperative nature. Concerning the Coulomb explosion experiments, it was pointed out that the 7-azaindole+H⁺ mass-119 species can be generated by the proton transfer after ionization (26). Especially, a recent theoretical calculation of Chen and Chao (43) showed that the efficient single-proton transfer takes place in the 7-azaindole dimer cation and anion, which is consistent with this argument.

Consequently, also for the gas-phase there is no experimental evidence that can support the existence of any detectable

intermediate during the double proton transfer process. Therefore, we can finally conclude that the double proton transfer reaction of the 7-azaindole dimer takes place with the concerted mechanism.

Concluding Remarks

Lastly, we mention the physical meaning of the concertedness to make our arguments clearer. So far, the debates about the double proton transfer mechanism have been made entirely for the viewpoint of whether the intermediate, in which only one proton is transferred, is observed as an identifiable transient species. Clearly, the present study provided solid experimental evidence that excludes the appearance of the intermediate species in between the dimer and tautomer excited states. Therefore, the step-wise mechanism was ruled out. Importantly, however, this conclusion does not necessarily translate to a synchronous motion for the two protons, in which they always move exactly the same distance, thereby preserving the C_{2h} symmetry of the dimer (44, 45). The synchronous manner is merely a special case of the concerted mechanism. The concerted mechanism, by its definition, does not require such a strict simultaneity, but it only means that the motions of the two protons are correlated. Actually, a recent molecular dynamics calculation for the formic acid dimer (46) suggested that the motion of the two protons can break the C_{2h} symmetry during the reaction, even though both the reactant and product have the C_{2h} symmetry. However, because such symmetry breaking was seen without a local minimum on the potential energy surface, the motion of the two protons cannot be considered separately. Therefore, this type of motion also is considered to be in the category of the concerted double proton transfer, even though the C_{2h} symmetry is broken

during the reaction. It is essentially different from the step-wise motion.

Experimental Procedures

The setup for femtosecond fluorescence up-conversion measurements was already reported (16, 21). Briefly, we used a femtosecond mode-locked Ti:sapphire laser (Tsunami; Spectra-Physics, Mountain View, CA) as a light source tunable in the 840- to 940-nm range. The third harmonic pulse (30 mW, 280–313 nm) was used as an excitation pulse, whereas the remaining fundamental component was used as a gate pulse for the up-conversion process. The fluorescence emitted from the sample was mixed with the gate pulse in a β -BaB₂O₄ crystal, and the up-converted signal was detected by a photon-counting system. The fluorescence detection at the magic angle was achieved by rotating the polarization of the excitation pulse. For anisotropy measurements, time-resolved fluorescence intensities with parallel and perpendicular conditions were measured at each delay time. The instrumental response time was evaluated as 290 fs by up-conversion measurements for instantaneous Raman signals of the solvent. 7-Azaindole (98%; Aldrich, St. Louis, MO) was recrystallized twice from cyclohexane and dried *in vacuo* before use. Liquid-chromatography grade hexane (Wako Pure Chemicals, Osaka, Japan) was used without further purification. A fresh sample solution (1×10^{-2} mol·dm⁻³) was prepared for each measurement. All of the fluorescence data were measured at room temperature (295 K).

S. T. was supported by Grant-in-Aid for Young Scientists B 17750026 from the Ministry of Education, Culture, Sports, Science, and Technology (Japan).

1. Arnaut LG, Formosinho SJ (1993) *J Photochem Photobiol A* 75:1–20.
2. Formosinho SJ, Arnaut LG (1993) *J Photochem Photobiol A* 75:21–48.
3. Waluk J (2003) *Acc Chem Res* 36:832–838.
4. Taylor CA, El-Bayoumi MA, Kasha M (1969) *Proc Natl Acad Sci USA* 63:253–260.
5. Ingham KC, Abu-Elgheit M, El-Bayoumi MA (1971) *J Am Chem Soc* 93:5023–5025.
6. Ingham KC, El-Bayoumi MA (1974) *J Am Chem Soc* 96:1674–1682.
7. El-bayoumi MA, Avouris P (1975) *J Chem Phys* 62:2499–2500.
8. Catalan J, Perez P (1979) *J Theor Biol* 81:213–221.
9. Waluk J, Bulska H, Pakula B, Sepiol J (1981) *J Lumin* 24/25:519–522.
10. Bulska H, Grabowska A, Pakula B, Sepiol J, Waluk J, Wild UP (1984) *J Lumin* 29:65–81.
11. Fuke K, Yoshiuchi H, Kaya K (1984) *J Phys Chem* 88:5840–5844.
12. Tokumura K, Watanabe Y, Udagawa M, Itoh M (1987) *J Am Chem Soc* 109:1346–1350.
13. Fuke K, Kaya K (1989) *J Phys Chem* 93:614–621.
14. Hetherington WM, III, Micheels RH, Eisenthal KB (1979) *Chem Phys Lett* 66:230–233.
15. Share P, Pereira M, Sarisky M, Repinec S, Hochstrasser RM (1991) *J Lumin* 48/49:204–208.
16. Takeuchi S, Tahara T (1998) *J Phys Chem A* 102:7740–7753.
17. Catalan J, Kasha M (2000) *J Phys Chem A* 104:10812–10820.
18. Sekiya H, Sakota K (2006) *Bull Chem Soc Jpn* 79:373–385.
19. Douhal A, Kim SK, Zewail AH (1995) *Nature* 378:260–263.
20. Folmer DE, Poth L, Wisniewski ES, Castleman AW, Jr (1998) *Chem Phys Lett* 287:1–7.
21. Takeuchi S, Tahara T (1997) *Chem Phys Lett* 277:340–346.
22. Chachisvilis M, Fiebig T, Douhal A, Zewail AH (1998) *J Phys Chem A* 102:669–673.
23. Fiebig T, Chachisvilis M, Manger MM, Zewail AH (1999) *J Phys Chem A* 103:7419–7431.
24. Catalan J, del Valle JC, Kasha M (1999) *Proc Natl Acad Sci USA* 96:8338–8343.
25. Folmer DE, Wisniewski ES, Castleman AW, Jr (2000) *Chem Phys Lett* 318:637–643.
26. Catalan J, del Valle JC, Kasha M (2000) *Chem Phys Lett* 318:629–636.
27. Douhal A, Moreno M, Lluch JM (2000) *Chem Phys Lett* 324:75–80.
28. Douhal A, Moreno M, Lluch JM (2000) *Chem Phys Lett* 324:81–87.
29. del Valle JC, Kasha M, Catalan J (2000) *Int J Quantum Chem* 77:118–127.
30. Moreno M, Douhal A, Lluch JM, Castano O, Frutos LM (2001) *J Phys Chem A* 105:3887–3893.
31. Catalan J, Perez P, del Valle JC, de Paz JL, Kasha M (2002) *Proc Natl Acad Sci USA* 99:5793–5798.
32. Catalan J, Perez P, del Valle JC, de Paz JL, Kasha M (2002) *Proc Natl Acad Sci USA* 99:5799–5803.
33. Catalan J, Perez P, del Valle JC, de Paz JL, Kasha M (2004) *Proc Natl Acad Sci USA* 101:419–422.
34. Douhal A, Guallar V, Moreno M, Lluch JM (1996) *Chem Phys Lett* 256:370–376.
35. Guallar V, Batista VS, Miller WH (1999) *J Chem Phys* 110:9922–9936.
36. Catalan J, de Paz JL (2005) *J Chem Phys* 123:114302.
37. Takeuchi S, Tahara T (2001) *Chem Phys Lett* 347:108–114.
38. Catalan J (2002) *J Phys Chem A* 106:6738–6742.
39. Sakota K, Hara A, Sekiya H (2004) *Phys Chem Chem Phys* 6:32–36.
40. Sakota K, Sekiya H (2005) *J Phys Chem A* 109:2718–2721.
41. Sakota K, Sekiya H (2005) *J Phys Chem A* 109:2722–2727.
42. Sakota K, Okabe C, Nishi N, Sekiya H (2005) *J Phys Chem A* 109:5245–5247.
43. Chen HY, Chao I (2004) *Chem Phys Chem* 5:1855–1863.
44. Chen Y, Gai F, Petrich JW (1993) *J Am Chem Soc* 115:10158–10166.
45. Catalan J, Diaz C, Perez P, de Paz JL (2006) *J Phys Chem A* 110:9116–9122.
46. Ushiyama H, Takatsuka K (2001) *J Chem Phys* 115:5903–5912.